Journal of Energy Storage 82 (2024) 110585

Contents lists available at ScienceDirect

Journal of Energy Storage

journal homepage: www.elsevier.com/locate/est

Research papers

Hydrogen storage potential of salt domes in the Gulf Coast of the United States

Leopoldo M. Ruiz Maraggi *, Lorena G. Moscardelli

Bureau of Economic Geology, The University of Texas at Austin, United States of America

ARTICLE INFO

Keywords:
Hydrogen geologic storage
Hydrogen storage evaluation
Salt caverns
U.S. salt domes

ABSTRACT

Hydrogen (H_2) has the potential to become a clean fuel alternative to replace hydrocarbons in a low-carbon economy with H_2 storage representing a key component of the emerging H_2 value chain. However, the use of H_2 for bulk power management and other industrial applications will require significant upscaling of geological storage. While geological H_2 storage can take place in both porous media and salt caverns within salt formations, salt caverns are considered the best option for underground H_2 storage for their large storage capacity, their sealing integrity, and their flexible operation with large injection and withdrawal rates. This study collects a comprehensive database of 569 salt domes located in the onshore and the offshore regions of the Gulf of Mexico Basin in the United States. This work filters the database by selecting onshore domes with no pre-existing caverns and a suitable depth range for salt cavern construction. As a result, we select and analyze 98 onshore salt domes suitable for H_2 storage in the states of Texas, Louisiana, and Mississippi. We perform H_2 storage capacity calculations for three scenarios: low, base, and high cases. For the base scenario, we estimate that these salt domes can accommodate a total of 2550 caverns, with a total working gas potential of 130 Gsm^3, equivalent to a total energy stored potential of 368 TWh. According to our base scenario, a 10 % replacement of the natural gas consumption in the United States, could require a H_2 storage capacity of 28 Gsm^3. This number implies the construction or repurposing of more than 556 salt caverns with a geometric volume of 0.75 Mm^3 per cavern. This study is the first of its kind, providing a breakdown of H_2 storage potential by state, county, and individual salt dome in the states of Texas, Louisiana, and Mississippi. The findings from this study provide valuable information for assessing the H_2 storage potential of salt domes in the United States, useful to assist in the definition of strategies to develop future H_2 infrastructure. Finally, we provide the readers with an interactive map that displays the results of this study.

1. Introduction

1.1. Motivation for underground hydrogen storage (UHS) in salt domes

The shift from fossil-based fuels to renewable energy is driving a major transformation in our energy systems, reshaping the way we consume energy. As part of this transition, H_2, a known carbon-free energy carrier, will play a vital role in bridging the gap between fossil fuels and renewables. However, to establish a successful H_2 economy, it is essential to develop several key components across the entire value chain including feedstock, production methods, storage, transportation, and marketability. For instance, to replace 10 % of the U.S. current natural gas consumption, which is equivalent to 915 Gsm^3 [1], could require a H_2 storage capacity of 28 Gsm^3. To reach this storage capacity, approximately 1000 salt caverns, each with a capacity of 28 Msm^3, would need to be either leached or adapted for H_2 storage. This estimate assumes a storage-to-consumption ratio of 10 % [2] and the energy content of H_2, measured in terms of its volumetric lower heating value, is one-third of natural gas. This simple calculation highlights the urgent need to scale up the H_2 storage capacity to unprecedented levels in order to achieve the goal of a net-zero economy within the next couple of decades. Currently, there are a limited number of salt cavern sites for H_2 storage in the United Kingdom (Teesside), and in the United States, including Clemens Dome, Spindletop, and Moss Bluff [3,4]. Clemens Dome has been in operation since 1983, while Moss Bluff began its operations in 2007 [4]. These long-standing projects have consistently shown the technical feasibility of underground H_2 storage. However, these subsurface H_2 storage facilities were not designed for bulk power management, industrial purposes (feedstock for steel and cement), or for

* Corresponding author.
E-mail address: leo.ruiz@beg.utexas.edu (L.M. Ruiz Maraggi).

https://doi.org/10.1016/j.est.2024.110585
Received 26 September 2023; Received in revised form 13 December 2023; Accepted 3 January 2024
Available online 25 January 2024

Nomenclature

d	cavern diameter, L, m
D	salt dome edge length, L, m
E_{cavern}	working gas energy per cavern, mL^2/t^2, TWh
E_{total}	total working gas energy, mL^2/t^2, TWh
f_{built}	fraction of caverns built, fraction
f_{loss}	volume fraction of brine and insolubles in the cavern, fraction
h	cavern height, L, m
L	edge length, L, m
M_{cavern}	mass per cavern, m, metric Ton
M_{total}	total mass, m, metric Ton
M_r	hydrogen molecular weight, m/mol, kg/kgmol
n	total number of caverns, number
n_{eff}	effective number of caverns, number
R	ideal gas constant, m L^2/(T t^2), J k^{-1} mol^{-1}
T	temperature, T, °C, K
V	volume, L^3, m^3
V_{cavern}	geometric volume of cavern, L^3, m^3
$V_{gas\ cavern}$	working gas volume per cavern at standard conditions, L^3, Msm^3
$V_{gas\ total}$	total working gas volume at standard conditions, L^3, Gsm^3
V_{total}	total geometric volume, L^3, m^3
Z	compressibility factor, dimensionless
z	Top of salt dome depth, L, m
ρ	density, m/L^3, kg/m^3

SI units prefixes

G	Giga, 10^9
k	Kilo, 10^3
M	Mega, 10^6
T	Tera, 10^{12}

transportation (fuel cells), and therefore, many challenges remain in terms of storage capacity upscaling, preservation of H_2 purity, and potential operational complications associated with high-frequency injection/withdrawal cycles.

The HyUnder project [5], funded by the European Union, assesses different large-scale options for underground H_2 storage, including salt caverns, porous media (depleted hydrocarbon reservoirs and aquifers), and lined rock caverns. Among these options, salt caverns are ranked as the most suitable choice for storing H_2 due to their integrity, compatibility with H_2, flexibility in withdrawal and injection rates, and cost-effectiveness. Currently, the European Union is supporting the Hypster project [6], which aims to demonstrate the combination of salt caverns for H_2 storage with renewable energy generation to promote decarbonization in industry and transportation. The Hypster project seeks to showcase the safety and minimal environmental impact of utilizing salt caverns for H_2 storage and power production, the pilot site is located in Etrez (France). The findings from the Hypster project will improve our understanding of favorable subsurface conditions for preserving H_2 quality and it will provide useful information to improve cost estimates associated with salt cavern H_2 storage.

1.2. Current capacity estimates

Numerous publications address the feasibility of salt cavern construction or repurposing for H_2 storage around the world. However, the vast majority of these publications focus on geological assessments or generalized aspects of the emerging H_2 economy without presenting calculations to estimate H_2 storage capacities using an engineering approach (Ozarslan. [7]; Iordache et al. [8]; Tarkowski and Czapowski [9]; Lewandowska-Śmierzchalska, J. et al., [10]; Deveci [11]; Lemieux et al. [12]; Zivar et al. [13]; among others). There are a few exceptions where efforts have been made to include more accurate H_2 storage assessment for salt caverns, the following studies are worth mentioning: 1) Michalski et al. [14] estimate that the total H_2 storage capacity in Northern Germany is about 26.5 TWh; 2) the HyUnder study [5] estimates a combined storage capacity of 133 GWh in Germany, the Netherlands, Spain, the United Kingdom, and Romania; 3) Caglayan et al. [15] assess the technical potential of salt caverns in domal salt and bedded salt formations across Europe estimating that the total onshore and offshore H_2 storage potential in Europe is 84.8 PWh; 4) Lankof et al. [16] estimate the H_2 storage capacity in the bedded salt formations of the Polish Zechstein Basin in 4.85 TWh; 5) Lankof et al. [17] update estimates in the Polish Zechstein Basin by incorporating storage capacity in the Mogilno salt dome adding an additional 125.7 TWh; 6) Liu et al. [18] perform calculations in the Jiangsu province in China estimating storage capacity around 36.9 TWh; 7) Williams et al. [19] assess the H_2 storage capacity of salt formations in the United Kingdom including the bedded salt formations located in the Cheshire Basin, East Yorkshire, and the Wessex Basin in 2150 TWh; and 8) Juez-Larré et al. [20] calculate the total H_2 storage capacity of the six salt caverns in the Zuidwending storage salt in 1.8 TWh. In the United States (U.S.) three studies are of relevance: 1) Simone et al. [21] provide an approximate evaluation of H_2 storage potential around 193 TWh for 93 onshore salt domes in the U.S. Gulf Coast while 2) Lackey et al. [22] estimate a total of 30 TWh of H_2 storage potential, mixed with natural gas, on existing U.S. salt caverns that currently store natural gas, and 3) Chen et al. [23] perform a study in the intermountain West region of the U.S. that included bedded and domal salt and estimating storage capacities between 26 and 38 million tons. The Simone et al. [21] contribution is relevant for this study since they are the first to provide an estimate for H_2 storage potential in the U.S. Gulf Coast. However, Simone et al. [21] do not include thermodynamic calculations in their study, this omission might impact the accuracy of their H_2 storage estimation. Accurate H_2 storage estimates are crucial to perform precise techno-economic evaluations since storage is a key element of the emerging H_2 value chain (Lin et al. [24]).

Regarding the cost of construction of salt caverns for H_2 storage, we provide some preliminary estimates from the following studies. In Poland, Tarkowski and Czapowski [9] estimate a cost of construction of caverns for storing 21 Msm^3 of H_2 of 25 million euros. Leighty [25] estimates that the cost of construction of the H_2 storage cavern with a 27 Msm^3 of working gas capacity in the Clemens dome located in Texas is around 20 million U.S. dollars.

1.3. Approach and new contributions

This study analyzes a comprehensive database of salt domes from the Gulf Coast region of the U.S. that include the states of Texas, Louisiana, and Mississippi [26–29] to assess their potential for H_2 storage using a novel thermodynamic simulator by Ruiz Maraggi and Moscardelli [30]. Input parameters for each salt dome include dome diameter and a suitable depth range for cavern placement (274 to 1676 m). This study presents a H_2 storage evaluation for three scenarios: low, base, and high cases. These scenarios differ in the cavern size, the cavern spacing, and the fraction of maximum number of caverns that can be built for each salt dome. Finally, this work breakdowns the results by state, county, and salt dome. The goals of this work are to perform a regional assessment for geological H_2 storage capacity and to identify areas where H_2 infrastructure investment could be prioritized based on proximity to potential storage sites.

These results should be taken as an initial H_2 storage assessment. Our approach is novel as it uses an in-house thermodynamic simulator to calculate H_2 storage capacities in salt caverns [30] while integrating real geoscience-based information from the subsurface [26–29]. In addition, we are using a geographic information system (GIS) approach to aid in the visualization of results, and the integration of other elements of the emerging H_2 value chain including proximity to relevant infrastructure, and potential markets (Scafidi et al. [31]; Lankof and Tarkowski [32]; Parkes, Williamson, and Williams [33]).

This work illustrates a study case for onshore salt domes located along the U.S. Gulf Coast. Finally, this approach can be easily applied to other salt formations, including bedded salt units, around the world.

2. Methods

This study uses the following steps to assess the technical potential of U.S. salt domes to store H_2.

1. Digitalization and geo-referencing of salt dome data from existing reports in the Gulf of Mexico region of the United States [26–29].
2. Definition of screening criteria and input parameters [30].
3. Calculation of storage capacities.

The first step involves the digitalization of previous publications from the Gulf Coast region of the United States including a United States Geological Survey (USGS) report [26], the Thieling and Moody study on the shallow Mississippi salt domes [27], a geological study of salt domes in southern Louisiana [28], and the Dellwig and Bare study of salt domes in northern Louisiana [29]. The digitalization of these reports involves building a database that includes: (a) state, (b) county, (c) geographical location, (d) federal information processing standards (FIPS) code, (e) salt dome depth (top of salt rock), and (f) salt dome average diameter for each salt dome. Subsequently, we incorporate this information to a geographical information system (GIS) database. To accomplish this goal, we use Folium [34], a Python [35] package suitable for geospatial data visualization and manipulation.

This study evaluates the storage potential of salt domes within a depth window between 274 and 1676 m for salt cavern construction. The minimum depth requirement (274 m) is set to prevent leakages [36,37] and for the cavern to be less susceptible to subsidence and seismic activities [36]. The maximum depth requirement (1676 m) is set to avoid salt creep which is the rate of deformation that occurs in a salt formation for a constant stress load. This phenomenon increases exponentially with depth and can cause major deformations and structural damage to salt caverns [38]. The depth range might vary depending on local subsurface conditions; however, the 274 to 1676 m depth window used in this study represents a sensible range.

Salt domes are abundant along the Gulf Coast of the United States, Gillhaus and Horvarth [39] present a comprehensive inventory of salt domes with pre-existing caverns in Texas, Louisiana, and Mississippi. However, this study excludes all salt domes with pre-existing caverns from the analysis since we want to evaluate the H_2 storage potential of salt domes with no previous commercial development. Finally, there are a number of salt domes within the original database without depth or diameter information that we exclude from the analysis.

Table 1 displays the input parameters for the assessment of H_2 storage capacity in salt domes for three different scenarios: low, base, and high cases. The differences between scenarios are: the geometric volume of caverns (0.50, 0.75, and 1 Mm^3 for low, base, and high scenarios, respectively), the adjacent cavern spacing (4, 3, and 2 cavern diameters, respectively), and the fraction of the maximum number of caverns that can be built within a salt dome (0.50, 0.55, and 0.60 for low, base, and high scenarios, respectively). The cavern geometric volumes for the low, base, and high scenarios reflect typical cavern sizes based on the literature [6,14] and actual caverns that store H_2 in the U.S. For instance, the geometric volume of caverns that store H_2 in the Clemens, Moss Bluff, and Spindeltop domes are 0.58, 0.57, and 0.90 Mm^3, respectively [21].

Table 1
Input parameters to assess H_2 storage capacity in salt domes for low, base, and high scenarios. The differences between scenarios are: the geometric volume of caverns, the cavern spacing, and the fraction of the maximum number of caverns that can be built within a salt dome.

Parameter	Low Scenario	Base Scenario	High Scenario
Suitable depth range, [z_{min}, z_{max}] [m]	274–1676	274–1676	274–1676
Geothermal gradient, $\frac{dT}{dz}$ [°C/m]	0.027	0.027	0.027
Overburden pressure gradient, $\frac{dP_v}{dz}$ [kPa/m]	22.62	22.62	22.62
Maximum operating pressure gradient, $\frac{dP_{max}}{dz}$ [kPa/m]	19.23	19.23	19.23
Minimum operating pressure gradient, $\frac{dP_{min}}{dz}$ [kPa/m]	5.66	5.66	5.66
Cavern diameter, d [m]	61	61	61
Cavern height, h [m]	174	261	349
Cavern geometric volume, V_{cavern} [Mm^3]	0.50	0.75	1
Edge length (distance between adjacent caverns), L [m]	244	183	122
Fraction brine & insolubles, f_{loss} [fraction]	0.25	0.25	0.25
Fraction of caverns built, f_{built} [fraction]	0.50	0.55	0.60

Hydrogen storage capacity calculations use the following assumptions: (a) single-phase single component gaseous H_2 since H_2 is stored in salt caverns with 95 % purity [40] (b) perfect mixing, meaning that pressure and temperature are uniform within the cavern given that the pressure gradient in the cavern can be neglected due to the low density of H_2 and that the natural convection of H_2 in the cavern leads to a constant temperature, (c) H_2 acts as cushion gas, and (d) all caverns have the same cylindrical shape and volume for each scenario.

This study limits the maximum operating pressure gradient (19.23 kPa/m) to a fraction of 0.85 of the normal overburden pressure gradient (22.62 kPa/m) to prevent loss of containment due to hydraulic fracturing of the salt and/or cemented well casing. This value of the maximum operating pressure gradient is in accordance to the guidelines provided by the Texas Railroad Commission [41].

3. Storage capacity calculations

This section describes the mathematical formulas used to calculate the storage capacities of the onshore Gulf Coast salt domes.

3.1. Equation of State (EOS)

The estimation of H_2 compressibility factor (Z) and thus, density (ρ) are based on Lemmon et al. EOS [42].

$$Z(TP) = 1 + \sum_{i=1}^{9} a_i \left(\frac{100\ K}{T(K)}\right)^{b_i} \left(\frac{P(MPa)}{1\ MPa}\right)^{c_i}, \tag{1}$$

where a_i, b_i, c_i are the empirical coefficients of the correlation, see [42].

The real gas density uses Eq. (1) to estimate the H_2 compressibility factor Z.

$$\rho\ (T, P) = \frac{P\ Mr}{Z(T, P)\ RT}, \tag{2}$$

where R is the ideal gas constant (8.3145 J/mol^{-1} K^{-1}) and Mr is the molecular weight of H_2 (2.016 kg/kgmol).

Fig. 1 illustrates the validation of the used correlation against H_2 data from NIST [43] for different pressures and temperatures for H_2 (a) compressibility factor and (b) density.

3.2. Volumetric calculation

The volumetric calculation assumes that all caverns in a given salt dome have the same geometry. Given the geometry of the cavern and the salt dome, it computes the following variables: (a) number of salt caverns that can be built per salt dome, (b) geometric volume per cavern and total number of caverns, (c) working gas volume per cavern and total number of caverns, (d) H_2 combustion energy (based on the H_2 lower heating value) per cavern and total number of caverns, and (e) H_2 mass per cavern and total number of caverns. We compute these variables for each dome in the dataset based on reported salt dome depths and diameters. While salt dome geometries are generally more complex, our simple cylindrical geometry assumption serves the purpose of regional screening estimations.

Fig. 2 illustrates the key input geometric parameters for modeling H_2 storage in salt caverns and for performing the volumetric calculations. These geometrical parameters are: (a) salt dome diameter D, (b) cavern diameter d, (c) cavern height h, (d) edge length L (distance between centers of adjacent caverns).

3.2.1. Total number of caverns

Eq. (3) computes the total number of caverns n, given the salt dome diameter D, the cavern diameter d, and the edge length L (see Fig. 2). This variable is the maximum number of caverns that can be built within a salt dome.

$$n(D,d,L) = \frac{\pi\left[\frac{(D-2d)}{2} - \sqrt{1/2}\,L\right]^2}{L^2}. \tag{3}$$

Fig. 2 shows that caverns are circumscribed within squares and the salt dome perimeter is modeled as a circle. To determine the number of squares (caverns) that can fit in a circle (salt dome), we consider the relationship between the dimensions of the square and the circle. The size of the square that can fit inside a circle is determined by the radius of the circle. One key formula to remember is that the side length of the largest square that can fit inside a circle is given by $\sqrt{2}$ radius of the circle. This formula comes from the fact that the diagonal of the square is equal to the diameter of the circle. Using the Pythagorean theorem in a 45-45-90 right triangle, where each leg of the triangle is a side of the square and the hypotenuse is the diameter of the circle, gives this relationship.

3.2.2. Effective number of caverns

Eq. (4) calculates the effective number of caverns n_{eff}, given the total number of caverns n and the fraction of caverns being built f_{built}, this parameter is defined for each scenario in Table 1. The effective number of caverns is a fraction of the total number of caverns.

$$n_{eff} = f_{built}\, n. \tag{4}$$

3.2.3. Total geometric volume of caverns

The total geometric volume of caverns is the multiplication of the geometric volume of a cavern V_{cavern} by the effective number of caverns n_{eff}. The total geometric volume is the summation of the geometric volume of the number of caverns that can be built inside a salt dome.

$$V_{total} = n_{eff}\, V_{cavern}. \tag{5}$$

3.2.4. Working gas volume per cavern

The working gas volume of a cavern is the gas volume at standard conditions that can be withdrawn or injected (total gas volume minus cushion gas volume).

$$V_{gas\ cavern} = \frac{1}{\rho(T_{std}, P_{std})}\left[\rho(T_{cavern}, P_{max}) - \rho(T_{cavern}, P_{min})\right](1-f_{loss})\, V_{cavern}, \tag{6}$$

where P_{max} and P_{min} are the maximum and minimum operating pressures corresponding to the maximum and minimum pressure gradient of Table 1 evaluated at the casing shoe depth (top salt depth plus hanging wall): $z + 0.75d$ (see Fig. 2b). The cavern temperature T_{cavern} is evaluated using the geothermal gradient in Table 1 at a depth equal to half of the height of the cavern: $z + 0.75d + 0.5h$. This study uses the following values for standard conditions: 15 °C and 1 atm.

3.2.5. Total working gas volume

The total working gas volume is the multiplication of the working gas volume of a cavern $V_{gas\ cavern}$ by the effective number of caverns n_{eff}. The total working volume is the summation of the working gas volume for the number of caverns that can be built inside a salt dome.

$$V_{gas\ total} = n_{eff}\, V_{gas\ cavern}. \tag{7}$$

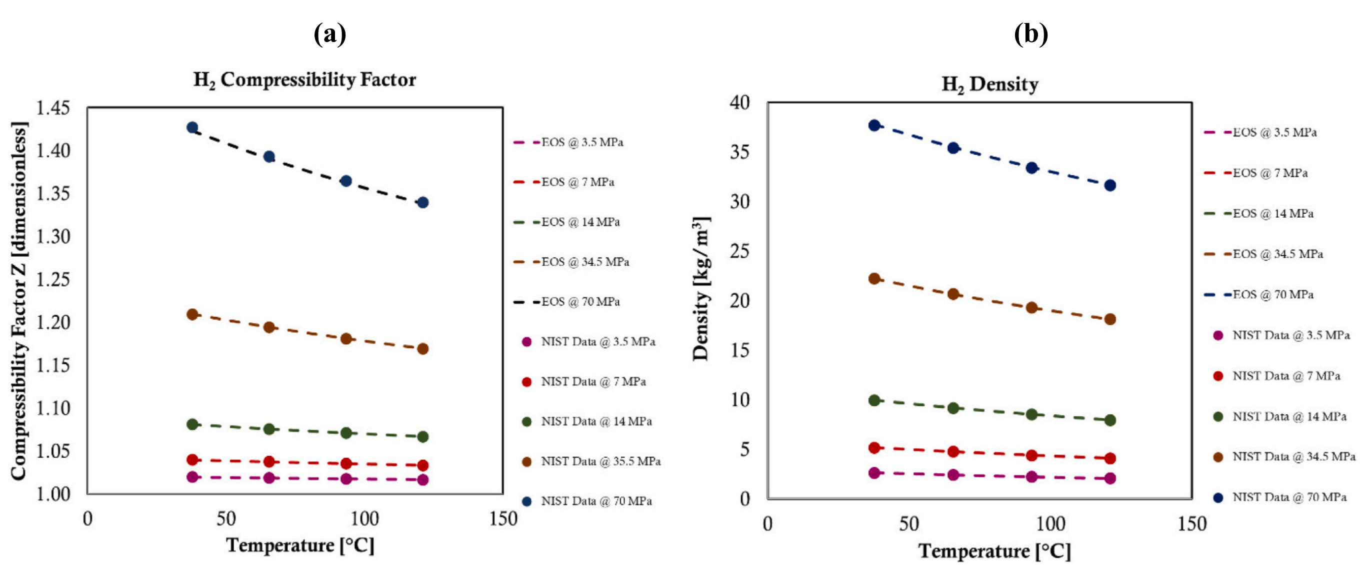

Fig. 1. Validation of the used correlation [42] (dashed curves) with H_2 data (solid dots) from the National Institute of Standards and Technology [43]: (a) compressibility factor and (b) density.

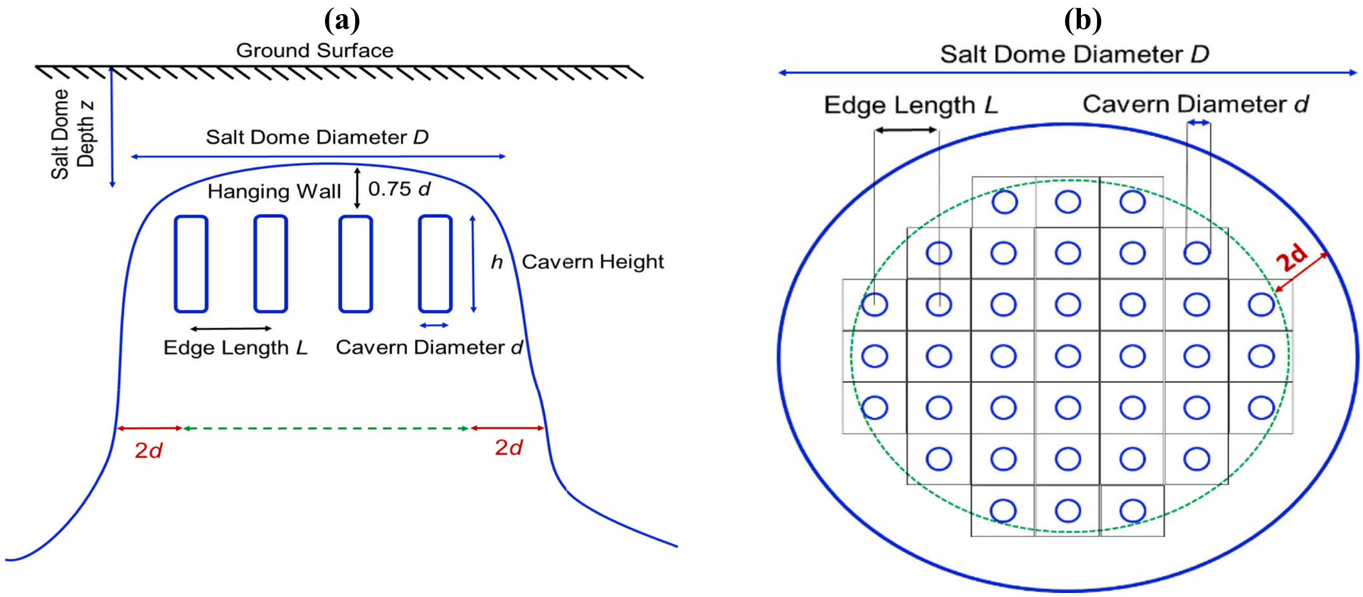

Fig. 2. Schematic illustrating salt caverns in a salt dome: (a) lateral view and (b) top view. The input geometric parameters for the volumetric calculations are: (a) salt dome diameter *D*, (b) cavern diameter *d*, (c) cavern height *h*, (d) edge length *L* (distance between centers of adjacent caverns).

3.2.6. Energy per cavern

The energy per cavern is the combustion energy of the working gas volume based on the lower heating value (*LHV*) per unit volume of H_2 (10.8 MJ/sm^3). Reference conditions for the evaluation of the *LHV* are 25 °C and 1 atm.

$$E_{cavern} = V_{gas\ cavern}\, LHV \left[\frac{\rho(25^{\circ}\mathrm{C}, P_{std})}{\rho(T_{std}, P_{std})}\right]. \tag{8}$$

3.2.7. Total energy

The total energy is the multiplication of the energy per cavern $V_{gas\ cavern}$ by the effective number of caverns n_{eff}.

$$E_{total} = n_{eff}\, E_{cavern}. \tag{9}$$

3.2.8. Mass per cavern

The mass per cavern is the mass of the working gas volume, which is the multiplication of the standard density ρ_{std} (standard conditions: 15 °C and 1 atm) by the working gas volume.

$$M_{cavern} = \rho(T_{std}, P_{std})\, V_{gas\ cavern}. \tag{10}$$

3.2.9. Total mass

The total mass is the multiplication of the mass per cavern M_{cavern} by the effective number of caverns n_{eff}.

$$M_{total} = n_{eff}\, M_{cavern}. \tag{11}$$

4. Results

This section presents the results of the analysis of the salt dome database from the southern region of the United States including the states of Texas, Louisiana, and Mississippi. Fig. 3 displays the geographic location of 569 salt domes compiled from multiple sources as described in the methods section [24–27]. This database includes domes from four distinctive salt tectonic domains in the southern United States including the Central Louann, East Texas, North Louisiana, and Mississippi salt basins (Fig. 3a). Salt domes in the Central Louann salt basin include both onshore and offshore domes. Domes in the onshore Central Louann salt basin are scarce in south Texas; however, their abundance increases toward the northeast along the Gulf Coast region (Fig. 3a). Fig. 3b shows number of salt domes by region, the offshore region of the Gulf of Mexico (GOM) basin has the highest count of salt domes (287) followed onshore by the states of Louisiana (130), Texas (90), and Mississippi (62). Figs. 3c and 3d illustrate the distributions of salt dome depth and salt dome diameter by region, respectively. The average salt dome depth is approximately 1011 m in Texas, 1645 m in Louisiana, 1272 m in Mississippi, and 1880 m in the offshore region of the GOM. The average salt dome diameter is approximately 2026 m in Texas, 1241 m in Louisiana, 1852 m in Mississippi, and 1976 m in the offshore region of the GOM. It is worth noting that the distribution of salt dome depths and diameters exhibits the largest variability in the offshore region of the GOM and the smallest variability in onshore Mississippi. This last observation relates to the level of complexity and deformation that salt masses present in offshore regions compared to the onshore component of the greater GOM basin (e.g.: salt canopies, suture zones, etc.).

Fig. 4 presents a choropleth map with the density of salt domes by county in the states of Texas, Louisiana, and Mississippi (Fig. 4a). The color variations on the map convey the density of the number of salt domes by county. Figs. 4b, 4c, and 4d illustrate the top 10 counties in Texas, Louisiana, and Mississippi that have the largest number of salt domes. In each state, the counties with the largest number of salt domes are: Anderson (Texas) with 8, Plaquemines (Louisiana) with 11, and Hinds (Mississippi) with 6 salt domes, respectively.

Fig. 5 illustrates the geographic location of the 98 onshore salt domes that have a suitable required depth range for salt cavern construction (274–1676 m), have no pre-existing caverns, and have enough data to estimate an average diameter (Fig. 5a). Fig. 5b shows number of salt domes by region, Mississippi has the largest number of salt domes under study (44) followed by Texas (28), and Louisiana (26). Figs. 5c and 5d show the distributions of salt dome depth and salt dome diameter by region, respectively. The average salt dome depth is approximately 801 m in Texas, 741 m in Louisiana, and 844 m in Mississippi. The average salt dome diameter is approximately 1870 m in Texas, 1237 m in Louisiana, and 1781 m in Mississippi.

Table 2 presents the results of the volumetric calculations for the 98 salt domes under study for the low, base, and high scenarios. For the purpose of comparison, this table also includes the Simone et al. assessment [21], which uses the USGS report [26] to perform its estimation. The Simone et al. [21] study provides an estimate that falls between the results of our low and base scenarios. It is important to note the differences between their assessment and this study. Simone et al.

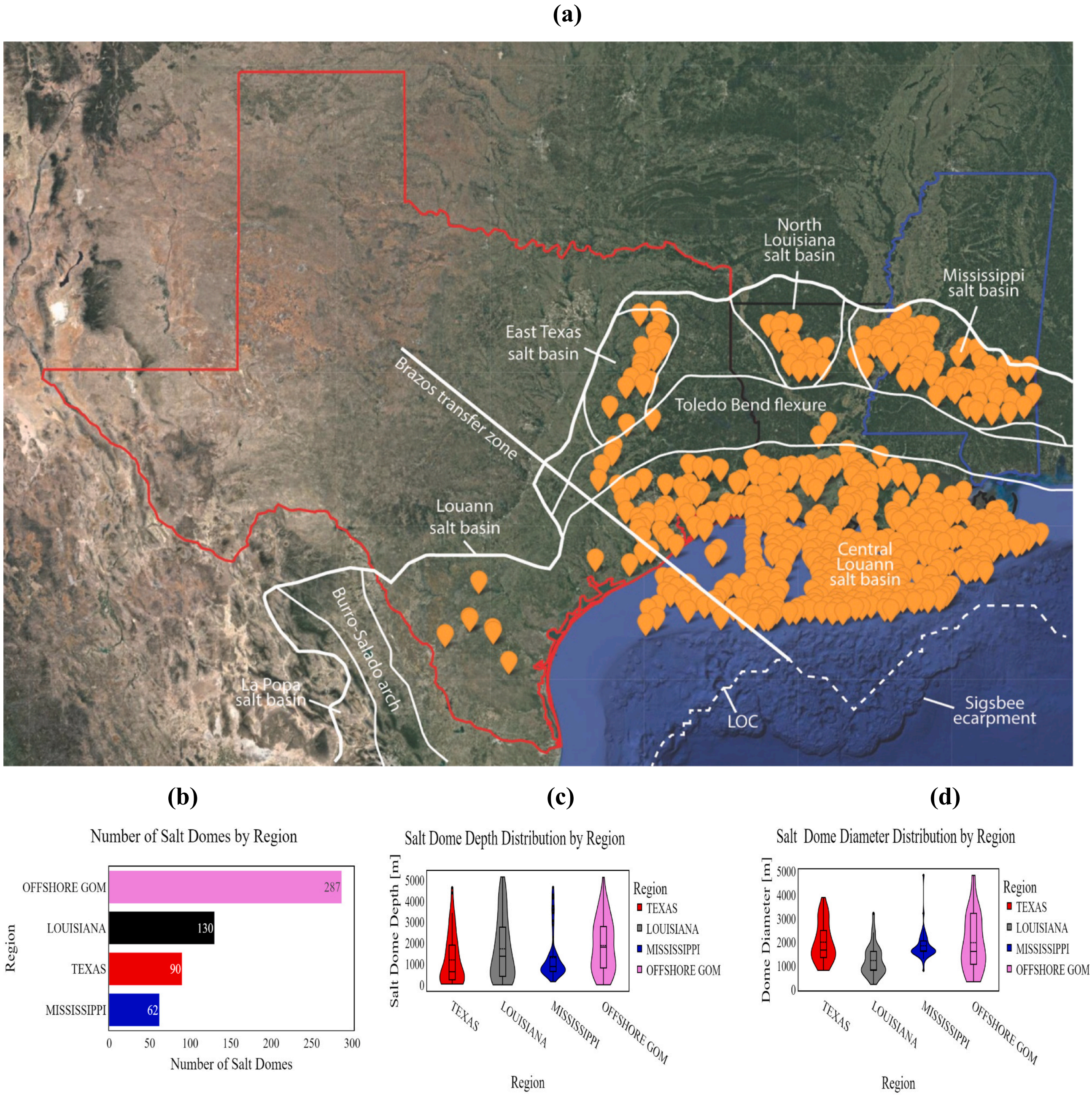

Fig. 3. Geographic location of 569 salt domes in the southern United States including the Central Louann, East Texas, North Louisiana, and Mississippi salt basins (Fig. 3a). Fig. 3b shows the number of salt domes by region. Figs. 3c and 3d illustrate the distributions of salt dome depth and salt dome diameter by region, respectively. The average salt dome depth is approximately 1011 m in Texas, 1645 m in Louisiana, 1272 m in Mississippi, and 1880 m in the offshore GOM. The average salt dome diameter is approximately 2026.31 m in Texas, 1241 m in Louisiana, 1852 m in Mississippi, and 1976 m in the offshore GOM..

[21] use an average working gas volume and an average salt dome diameter to perform their estimation. In contrast, this work calculates the number of caverns and working gas volume for each salt dome individually, considering both the specific depth and diameter of each salt dome. Furthermore, this study accounts for H_2 fluid properties with pressure and temperature using thermodynamic calculations [30].

Fig. 6 provides a detailed breakdown of the results for the low, base, and high scenarios (Table 2) for the states of Texas, Louisiana, and Mississippi. The breakdown includes the following aspects: (a) number of caverns, (b) working gas volume, (c) H_2 energy, and (d) H_2 mass. The analysis reveals that Mississippi has the largest potential for geological H_2 storage, followed by Texas and Louisiana. These findings align with the results presented in Fig. 5b, as Mississippi has the largest number of domes under study.

Fig. 7 displays a choropleth map that shows the number of salt caverns by county in Texas, Louisiana, and Mississippi. This information corresponds to the base scenario in Table 2. The varying colors on the map represent the density of caverns for each county. Fig. 7 also highlights the top 10 counties in Texas, Louisiana, and Mississippi that have the potential to accommodate the largest number of caverns. Specifically, Anderson County in Texas has the potential to accommodate 211 caverns, Lafourche County in Louisiana 111 caverns, and Lamar County in Mississippi 165 caverns. The names of the top 10 domes in Texas, Louisiana, and Mississippi with potential to develop the largest number of caverns are also provided. The domes with potential to accommodate the largest number of caverns in each state are: Boggy Creek dome in

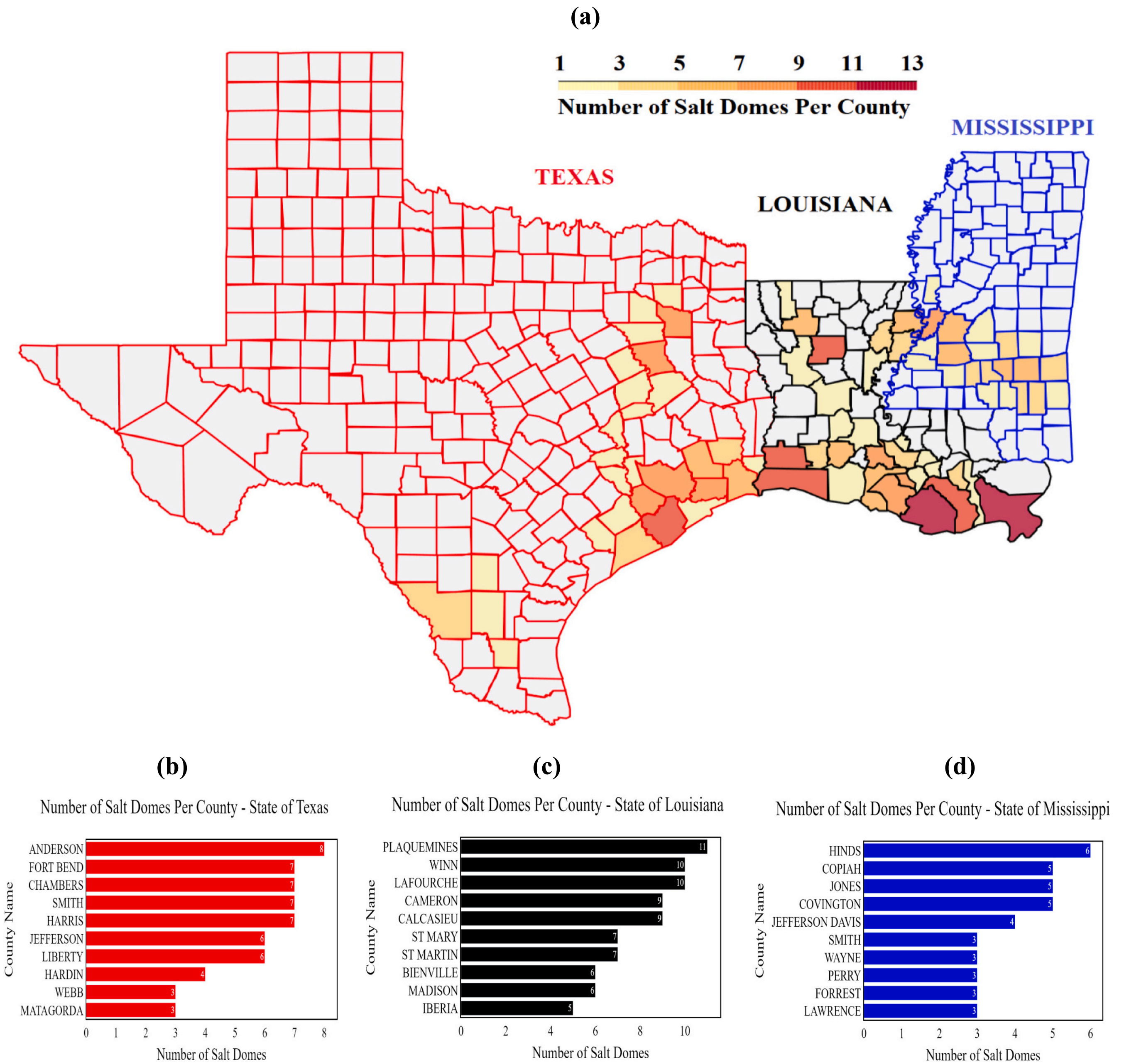

Fig. 4. Choropleth map illustrating the salt dome density by county in Texas, Louisiana, and Mississippi. The color variations on the map represent the number of salt domes by county. Figs. 4b, 4c, and 4d illustrate the top 10 counties in Texas, Louisiana, and Mississippi that have the largest number of salt domes. In each state, the counties with the largest number of salt domes are: Anderson (Texas) with 8, Plaquemines (Louisiana) with 11, and Hinds (Mississippi) with 6 salt domes, respectively.

Anderson County (Texas) with 158 caverns, Chacahoula dome in Lafourche County (Louisiana) with 103 caverns, and Tatum dome in Lamar County (Mississippi) with 103 caverns.

The counties with the largest potential for working gas capacity in our base scenario (Table 2) for each state are: Anderson in Texas with 27.8 TWh, Lafourche in Louisiana with 8.4 TWh, and Warren in Mississippi with 31.3 TWh (Fig. 8). In terms of individual domes, the domes with the largest potential for H_2 energy storage in each state are: La Rue in Henderson County (Texas) with a capacity of 26.7 TWh, Chacahoula in Lafourche County (Louisiana) with a capacity of 7.71 TWh, and Tatum in Lamar County (Mississippi) with a capacity of 9.73 TWh (Fig. 8).

5. Discussion

If H_2 were to replace 10 % of the U.S. annual natural gas consumption, which is equivalent to 915 Gsm^3 [1], then 28.32 Gsm^3 of H_2 storage capacity would be required. This calculation assumes a 10 % storage versus consumption ratio [2]. Our base scenario suggests that a storage capacity of 28.32 Gsm^3 would require the construction or repurposing of more than 556 salt caverns with a geometric volume of 0.75 Mm^3 per cavern and 80 TWh of stored energy. It is important to highlight that individual salt cavern construction can take several years from planning to completion, and that engaging in new salt cavern construction involves large capital expenditures. Lackey et al. [22] suggests that the repurposing of existing underground gas storage (UGS) facilities can significantly decrease the initial capital investment associated with new

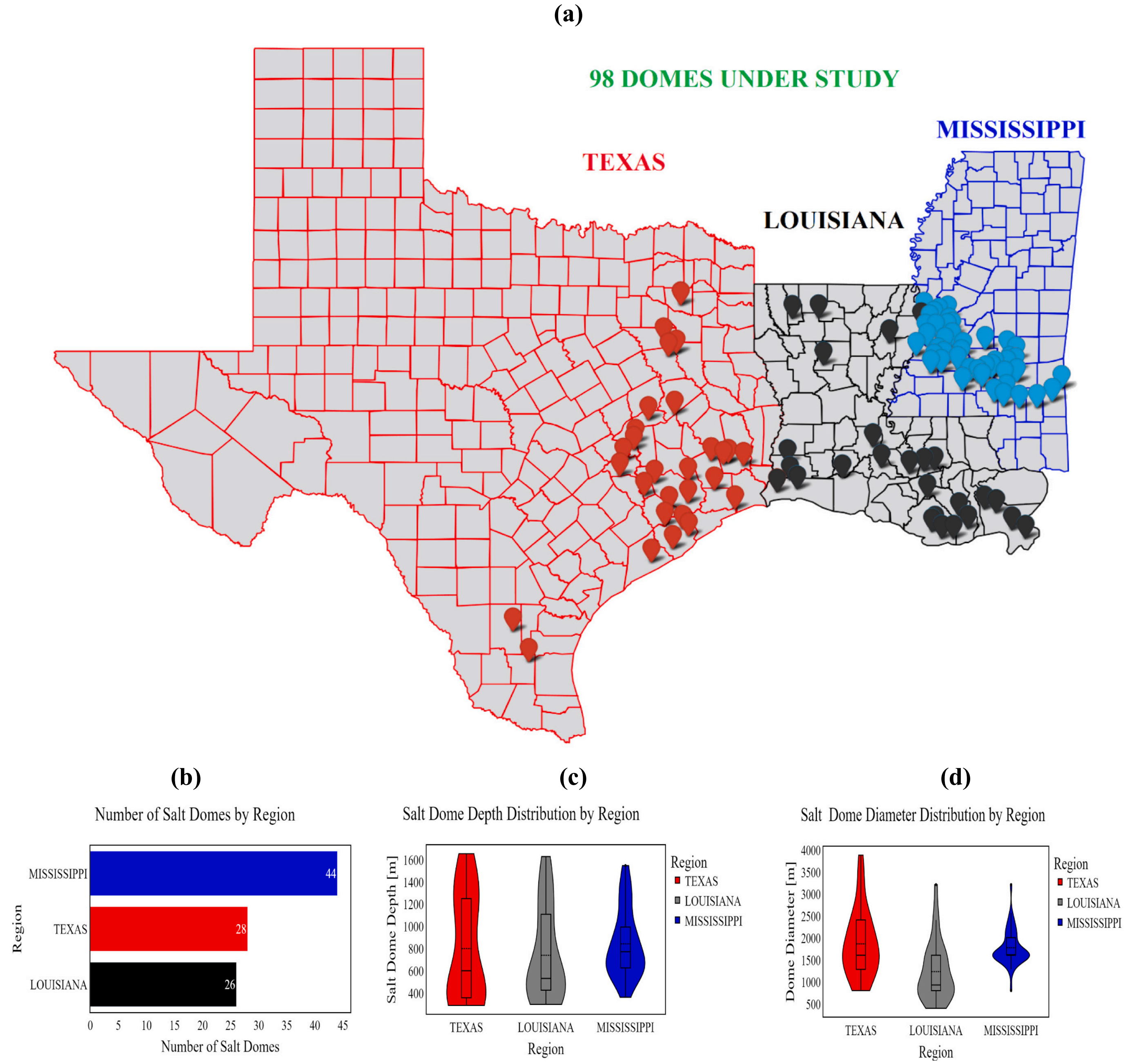

Fig. 5. Geographic location of the 98 salt domes under study in onshore Texas, Louisiana, and Mississippi (Fig. 5a). The map shows the location of salt domes by county in these states. These salt domes are within the 274–1676 m depth range where salt cavern construction is feasible (see Table 1), have no pre-existing caverns, and have enough data to estimate an average dome diameter. Fig. 5b shows number of salt domes by region. Mississippi has the largest number of suitable salt domes (44) followed by Texas (28), and Louisiana (26).

H_2 infrastructure. However, their estimate of H_2 storage potential in existing UGS facilities, equivalent to 118 Gsm^3, is not enough to replace the U.S. natural gas consumption with H_2. A combination of new and repurposed infrastructure seems to present the best solution to progressively increase H_2 storage capacity as demand and markets evolve in the future.

This work estimates the H_2 storage potential of salt domes, assuming that caverns are perfectly cylindrical and considering hydrogen's fluid properties [30]. However, these estimates may not be fully accurate in real-world situations. Factors like hydrogen's chemical reactions, the impact of microbes, frequent changes in H_2 levels, potential weakening of materials (embrittlement), and the varied shapes of actual salt domes influence the storage capacity and operational efficiency of caverns. For this reason, the estimates of this study should be taken as an initial screening tool to flag domes and counties that have the largest H_2 storage potential within the Gulf Coast region. The combination of these estimates, based on subsurface conditions, and other elements that are part of the emerging H_2 value chain need to be incorporated into technoeconomic models to allow for the prioritization of development opportunities. Fig. 9 showcases an area of the Gulf Coast where our base scenario estimate for H_2 working gas capacity by county has been displayed in the background, the map also plots the location of key infrastructure that includes existing H_2 and CO_2 pipelines, refineries, and salt dome locations. This display brings light to the rationale behind some of the recent announcements associated with planned investments for H_2 hubs in the region. The development of the Louisiana Clean Energy

Table 2
Results of the volumetric calculations for the 98 onshore salt domes under study for the low, base, and high scenarios. For comparison purposes, this table also includes the Simone et al. assessment [21], which also uses the USGS report [25] to perform its estimations. The Simone et al. calculations fall between the results of our low and base scenarios.

Parameter	Low Scenario	Base Scenario	High Scenario	Simone et al. [21]
Domes under study	98	98	98	93
Individual cavern volume [Mm^3]	0.50	0.75	1.00	0.45
Number of caverns	1161	2550	7035	2790
Working gas [Gsm^3]	39.48	129.85	476.79	68.53
Energy [TWh]	112	368	1351	193.30
Mass [M metric Ton]	3.36	11.04	40.54	5.80

Complex has been announced with an investment of $4.5 billion, the project will take place in Ascension Parish where 21.24 Msm^3 of H_2 will be produced from natural gas [44]. Ascension Parish is strategically located in an area with access to CO_2 and H_2 pipelines, it also has favorable subsurface conditions for the permanent sequestration of CO_2 and the storage of H_2 in caverns within salt domes (Fig. 9). A different scheme has been proposed in the Mississippi Clean Hydrogen Hub [45], the plan is to produce an estimated 350 tons/day of renewable H_2 to fuel operations in the Port Bienville Industrial Park and the Stennis International Airport, and store more than 71,000 tons in salt caverns in Richton Dome. Our analysis highlights additional opportunities in areas of the Gulf Coast region that present the largest potential for H_2 storage in salt domes without existing caverns, these areas include the northern parts of Mississippi and Louisiana and the east of Texas.

6. Web-based interactive map application

We developed a web-based interactive map that illustrates the assessment of this paper. The use of the interactive map is only for illustration purposes. The reader can find the interactive map in the following url: https://www.beg.utexas.edu/research/programs/starr/hydrogen-storage

7. Conclusions

This is the first study to collect and provide comprehensive information associated with the H_2 storage potential for salt domes located in the onshore region of the Gulf Coast of the United States. This study considers 98 onshore salt domes with no previous cavern development and a depth range for cavern development between 274 and 1676 m. We present results by state, county, and individual salt dome to facilitate the analysis from regional to local scales. This study analyzes three scenarios: low, base, and high cases, with different cavern size, spacing, and density. The H_2 working gas and its stored energy potential range from 39.36 to 476.86 Gsm^3 and from 112 to 1351 TWh for the low and high scenarios. Achieving these low- and high-end scenarios would require the construction of 1161 and 7035 caverns with cavern geometric volumes ranging from 0.50 to 1 Mm^3 for the low- and high-end scenarios, respectively. For the low case scenario, the fraction of caverns built was only 50 % while for the high-end scenario it was 60 % so altering this assumption can greatly impact these estimates. The variables of our base case scenario are the most realistic in the short- to medium term if the

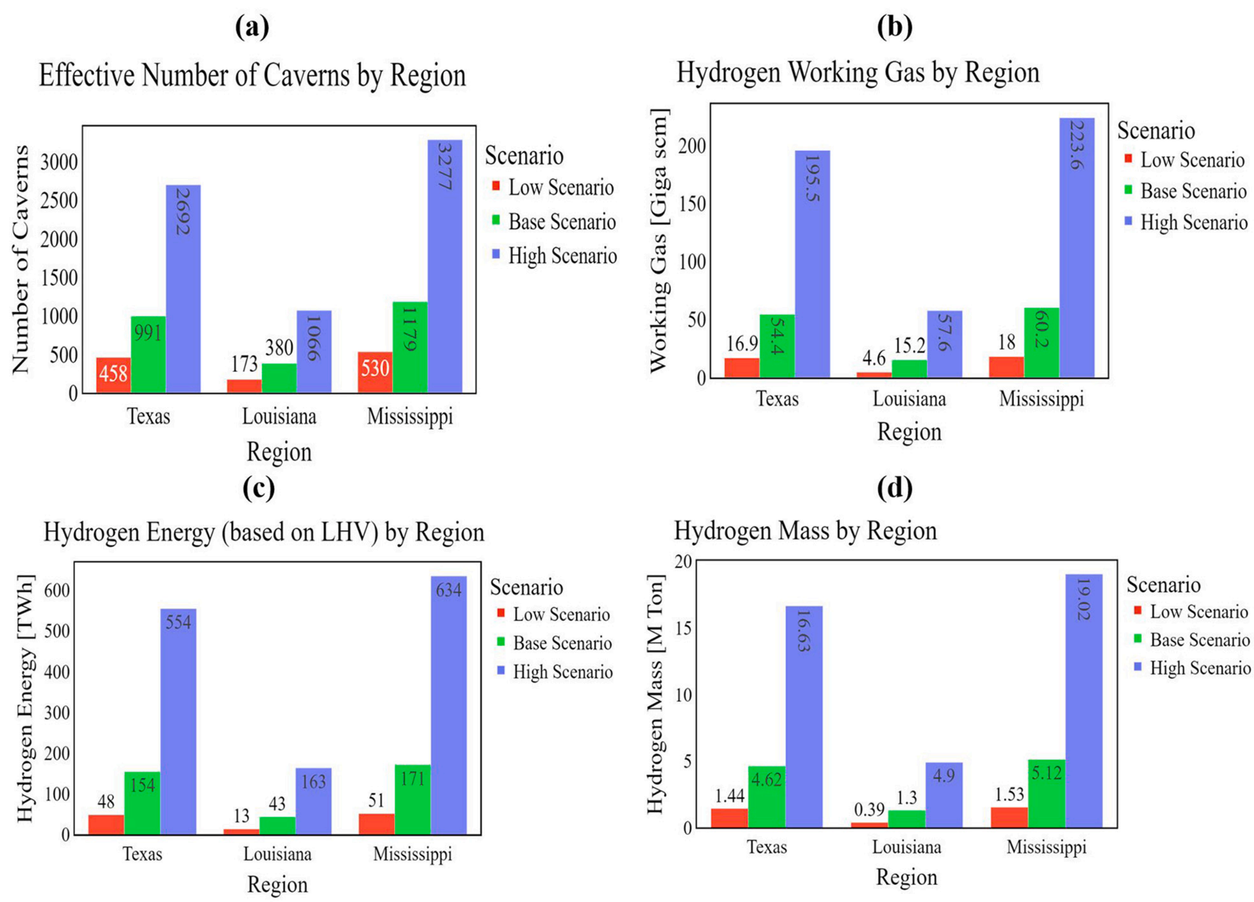

Fig. 6. Breakdown of results for the low, base, and high scenarios (Table 2) for the states of Texas Louisiana and Mississippi in terms of: (a) number of caverns, (b) working gas, (c) H_2 energy, and (d) H_2 mass. The analysis reveals that Mississippi has the largest potential for H_2 storage, followed by Texas and Louisiana. These findings align with the results presented in Fig. 5b, showing that Mississippi has the largest number of domes under study. LHV: Lower heating value.

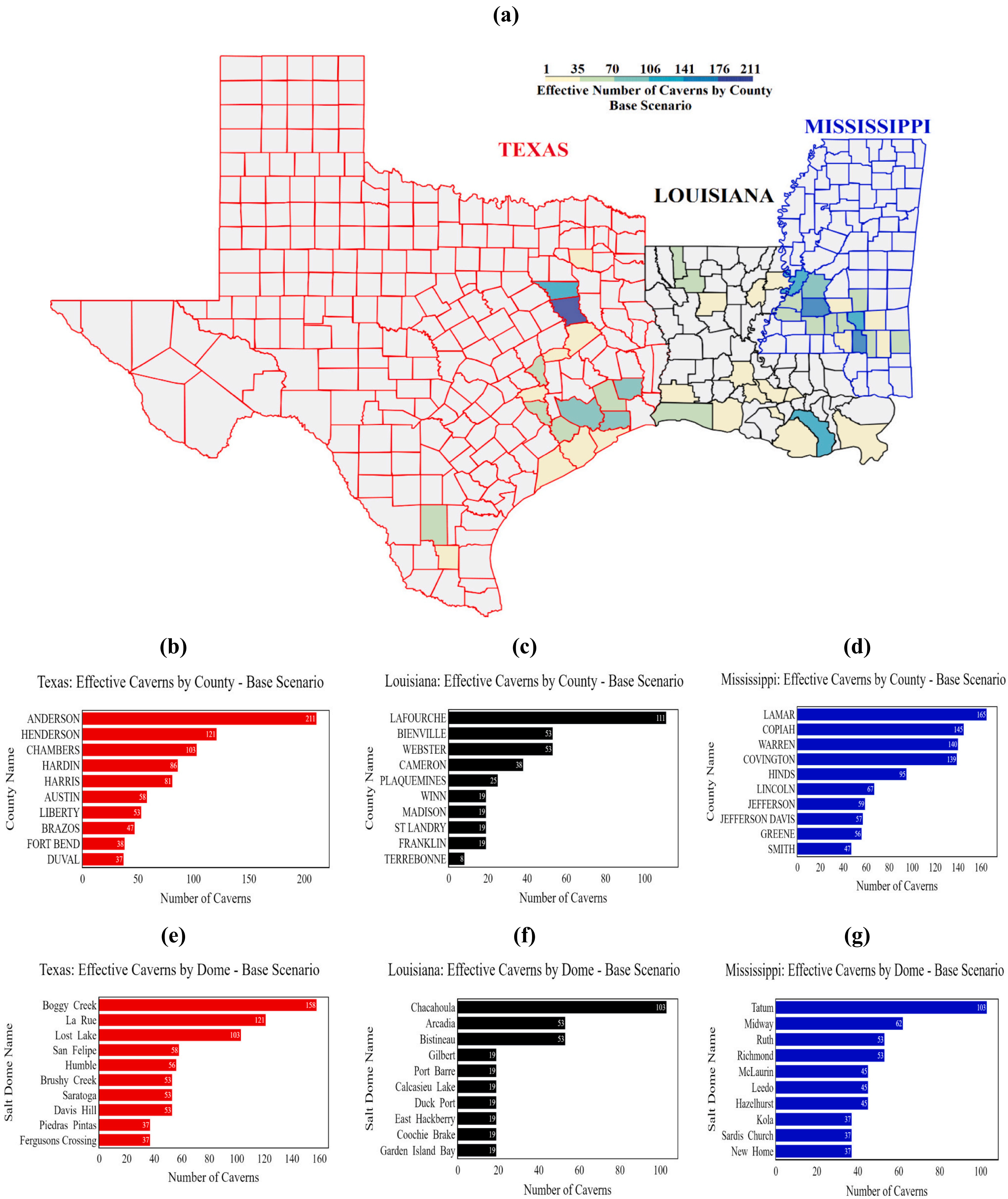

Fig. 7. Choropleth map illustrating the potential number of salt caverns that could be developed by county in Texas, Louisiana, and Mississippi (Fig. 7a). This information corresponds to our base scenario in Table 2. Figs. 7b, 7c, and 7d present the top 10 counties in Texas, Louisiana, and Mississippi that have the potential to accommodate the largest number of caverns. Figs. 7e, 7f, and 7 g show the top 10 domes in Texas, Louisiana, and Mississippi that have the potential to accommodate the largest number of caverns.

ambition is to replace at least 10 % of natural gas supply in the United States by 2050. In this case, we would need to build 556 salt caverns with a geometric volume of 0.75 Mm^3 per cavern to store 28.32 Gsm^3 of H_2 working gas, equivalent to 80 TWh of stored energy. However, given the high cost and time that are needed to leach new caverns, in addition to other technical considerations, it is unlikely that this 10 % replacement of natural gas by H_2 can be achieved exclusively by engaging in new salt cavern construction. A more realistic scenario to increase H_2 storage capacity in the Gulf Coast region will likely involve a combination of salt cavern repurposing, new salt cavern construction,

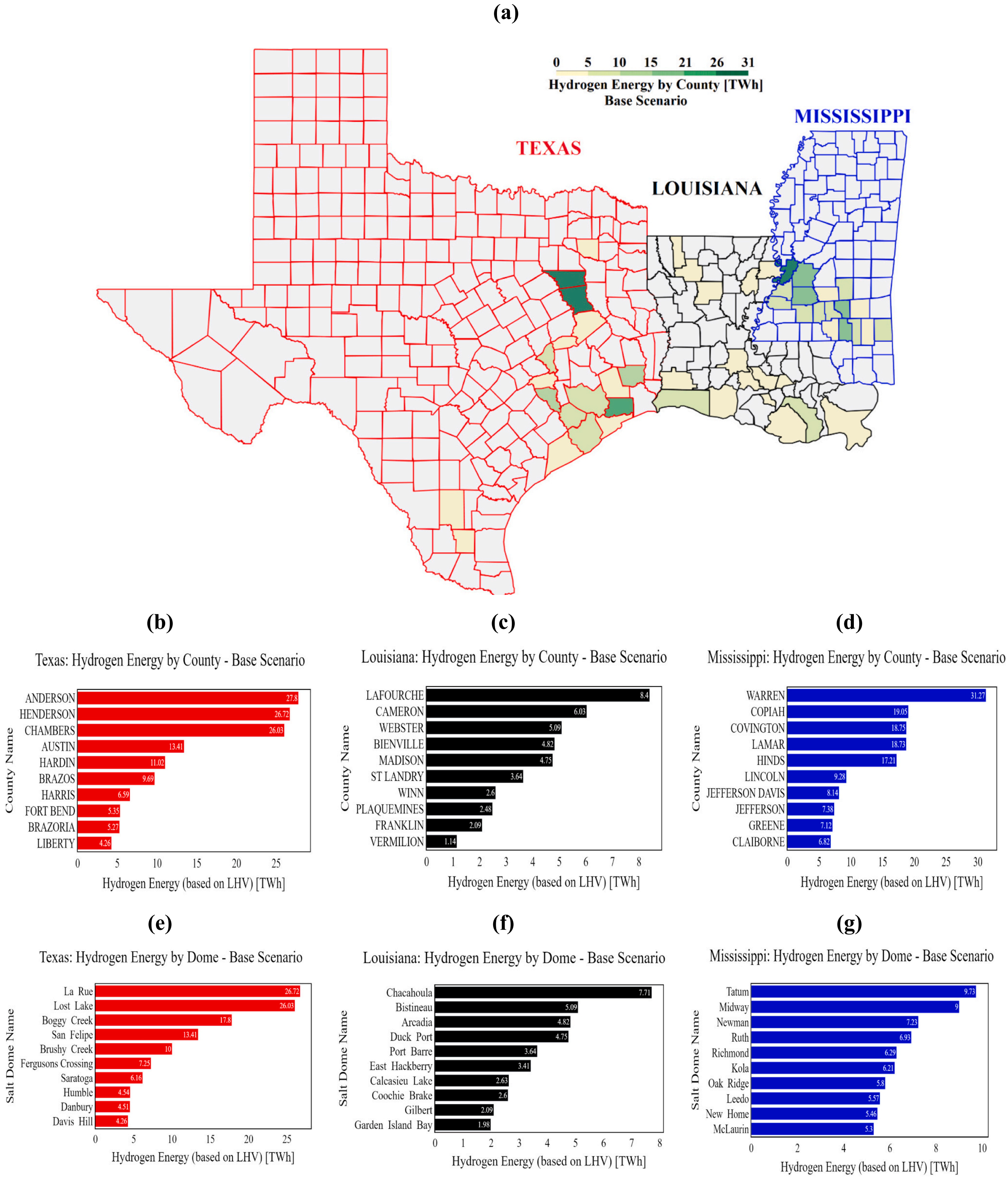

Fig. 8. Choropleth map illustrating the potential for H_2 energy density by county in Texas, Louisiana, and Mississippi (Fig. 9a). This information corresponds to the base scenario in Table 2. Figs. 8b, 8c, and 8d present the top 10 counties in Texas, Louisiana, and Mississippi with the largest potential for H_2 energy storage. Figs. 8e, 8f, and 8 g show the top 10 domes in Texas, Louisiana, and Mississippi with the largest potential for H_2 energy storage.

advances in H_2 storage in porous media, new construction of H_2 pipelines, as well as increase H_2 blending with natural gas so that existing infrastructure can be used to increase total storage capacity. Furthermore, our estimates suggest that Mississippi has the largest H_2 storage potential within the Gulf Coast region, followed by Texas and Louisiana. These results are based on the current available information regarding salt dome location, depth, and average diameter. The counties and parishes with the largest storage potential are: Anderson County in Texas, Lafourche Parish in Louisiana, and Warren County in Mississippi. This work is particularly useful to screen areas for the future

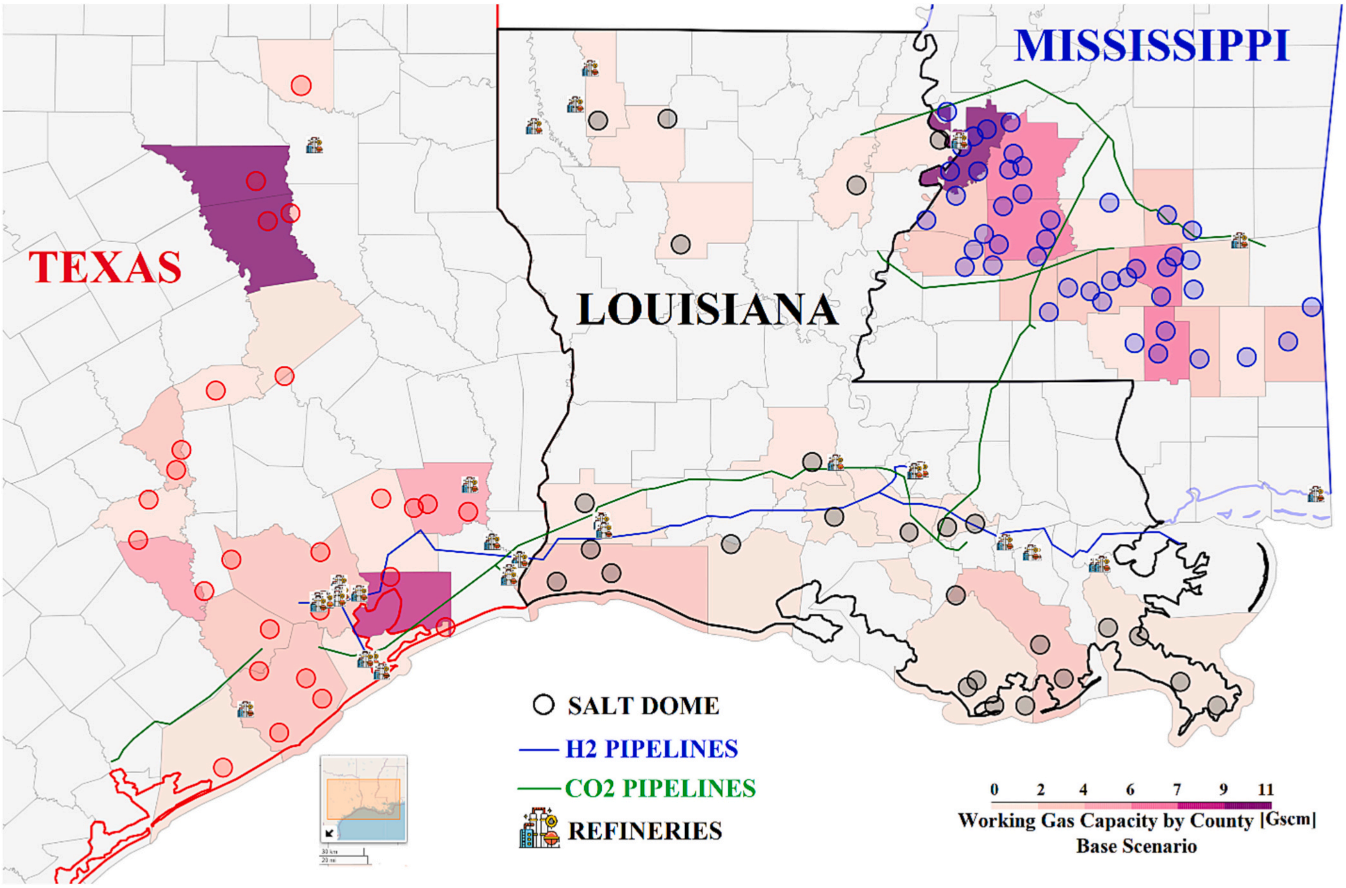

Fig. 9. Map illustrating salt domes and working gas capacity per county (base scenario) in the states of Texas, Louisiana, and Mississippi along with major H_2 and CO_2 pipelines, and refineries.

development of H_2 storage infrastructure. A more detailed analysis should consider a variety of surface and subsurface conditions that need to co-exist in order to develop a viable H_2 value chain. In addition to identifying potential subsurface H_2 storage sites, it is necessary to have proximity to feedstock, production methods, transportation, and markets.

CRediT authorship contribution statement

Leopoldo M. Ruiz Maraggi: Data curation, Formal analysis, Methodology, Software, Visualization, Writing – original draft, Writing – review & editing. **Lorena G. Moscardelli:** Project administration, Resources, Supervision, Writing – original draft, Writing – review & editing.

Declaration of competing interest

The authors declare that they have no known competing financial interests or personal relationships that could have appeared to influence the work reported in this paper.

Data availability

Data will be made available on request.

Acknowledgements

This work has been funded by the State of Texas Advanced Resource Recovery (STARR) program. The authors want to thank members of the GeoH$_2$ consortium at the Bureau of Economic Geology for supporting this work. The authors would like to thank Fredrik Saaf (Shell) for his comments, suggestions, and proofreading of this manuscript. Publication authorized by the director of the Bureau of Economic Geology, The University of Texas at Austin.

References

[1] U.S. Energy Information Administration, Natural Gas Annual Consumption. https://www.eia.gov/naturalgas/annual/, 2023.

[2] M. Shuster, S. Bhattacharya, I.J. Duncan, et al., Hydrogen infrastructure expansion requires realistic framework, Oil Gas J. 119 (5) (2021). https://www.ogj.com/pipelines-transportation/article/14202928/hydrogen-infrastructure-expansion-requires-realistic-framework.

[3] R. Tarkowski, Underground hydrogen storage: characteristics and prospects, Renew. Sustain. Energy Rev. 105 (2019) 86–94, https://doi.org/10.1016/J.RSER.2019.01.051.

[4] H. Landinger, F. Crotogino, The role of large-scale hydrogen storage for future renewable energy utilization, in: Second Int. Renew. Energy storage Conf. (IRES II), 2007.

[5] O. Kruck, F. Crotogino, Hyunder: Assessing the Potential, Actors, and Business Models of Large-Scale Underground Hydrogen Storage in Europe, Benchmark of selected storage options, http://hyunder.eu/wp-content/uploads/2016/01/D3.3_Benchmarking-of-selected-storage-options.pdf, 2013. (Accessed 15 March 2023).

[6] Hypster: hydrogen storage, Accessed March 15. https://hypster-project.eu/, 2023.

[7] A. Ozarslan, Large-scale hydrogen energy storage in salt caverns, Int. J. Hydrogen Energy 37 (2012) 14265–14277, https://doi.org/10.1016/j.ijhydene.2012.07.111.

[8] Iordache, et al., Hydrogen underground storage in Romania, potential directions of development, stakeholders and general aspects, Int. J. Hydrogen Energy 39 (2014) 11071–11081, https://doi.org/10.1016/j.ijhydene.2014.05.067.

[9] R. Tarkowski, G. Czapowski, Salt domes in Poland–Potential sites for hydrogen storage in caverns, Int. J. Hydrogen Energy 43 (2018) 21414–21427, https://doi.org/10.1016/j.ijhydene.2018.09.212.

[10] J. Lewandowska-Śmierzchalska, et al., Screening and ranking framework for underground hydrogen storage site selection in Poland, Int. J. Hydrogen Energy 43 (2018) 4401–4414, https://doi.org/10.1016/j.ijhydene.2018.01.089.

[11] M. Deveci, Site selection for hydrogen underground storage using interval type-2 hesitant fuzzy sets, Int. J. Hydrogen Energy 43 (2018) 9353–9369, https://doi.org/10.1016/j.ijhydene.2018.03.127.
[12] Lemieux, et al., Preliminary assessment of underground hydrogen storage sites in Ontario, Canada, Int. J. Hydrogen Energy 44 (2019) 15193–15204, https://doi.org/10.1016/j.ijhydene.2019.04.113.
[13] D. Zivar, S. Kumar, J. Foroozesh, Underground hydrogen storage: a comprehensive review, Int. J. Hydrogen Energy 46 (2021) 23436–23462, https://doi.org/10.1016/j.ijhydene.2019.04.113.
[14] J. Michalski, U. Bünger, F. Crotogino, S. Donadei, G.-S. Schneider, T. Pregger, et al., Hydrogen generation by electrolysis and storage in salt caverns: potentials, economics and systems aspects with regard to the German energy transition, Int. J. Hydrogen Energy 42 (2017) 13427–13443, https://doi.org/10.1016/j.ijhydene.2017.02.102.
[15] D.G. Caglayan, N. Weber, H.U. Heinrichs, et al., Technical potential of salt caverns for hydrogen storage in Europe, Int. J. Hydrogen Energy 45 (11) (2020) 6793–6805, https://doi.org/10.1016/j.ijhydene.2019.12.161.
[16] L. Lankof, R. Tarkowski, Assessment of the potential for underground hydrogen storage in bedded salt formation, Int. J. Hydrogen Energy 45 (38) (2020) 19479–19492, https://doi.org/10.1016/j.ijhydene.2020.05.024.
[17] L. Lankof, et al., Assessment of the potential for underground hydrogen storage in salt domes, Renew. Sustain. Energy Rev. 160 (2022) 112309, https://doi.org/10.1016/j.rser.2022.112309.
[18] Liu, et al., Feasibility evaluation of large-scale underground hydrogen storage in bedded salt rocks of China: a case study in Jiangsu province, Energy 198 (2020) 117348, https://doi.org/10.1016/j.energy.2020.117348.
[19] Williams, et al., Does the United Kingdom have sufficient geological storage capacity to support a hydrogen economy? Estimating the salt cavern storage potential of bedded halite formations, Journal of Energy Storage 53 (2022) 105109, https://doi.org/10.1016/j.est.2022.105109.
[20] Juez-Larré, et al., A detailed comparative performance study of underground storage of natural gas and hydrogen in the Netherlands, Int. J. Hydrogen Energy 48 (2023) 28843–28868.
[21] A. Simone, A. Morisani-Zechmeister, F. Frey, Preparing for a hydrogen future – constraints and alternatives for hydrogen storage, in: Solution Mining Research Institute Fall 2021 Technical Conference. 20-21 September, Galveston, TX, USA, 2021.
[22] G. Lackey, G.M. Freeman, T.A. Buscheck, F. Haeri, J.A. White, N. Huerta, A. Goodman, Characterizing hydrogen storage potential in U.S. underground gas storage facilities, Geophys. Res. Lett. 50 (3) (2023) 123–135, https://doi.org/10.1029/2022GL101420.
[23] F. Chen, et al., Capacity assessment and cost analysis of geologic storage of hydrogen: a case study in Intermountain-West Region USA, Int. J. Hydrogen Energy 48 (2023) 9008–9022, https://doi.org/10.1016/j.ijhydene.2022.11.292.
[24] N. Lin, L. Xu, L.G. Moscardelli, Market-based asset valuation of hydrogen geological storage, International Journal of Hydrogen Energy (2023), https://doi.org/10.1016/j.ijhydene.2023.07.074.
[25] W.C. Leighty, Running the world on renewables: hydrogen transmission pipelines with firming geologic storage, in: Proceedings of the ASME 2008 Power Conference. ASME 2008 Power Conference. Lake Buena Vista, Florida, USA. July 22–24, ASME, 2008, pp. 601–613, https://doi.org/10.1115/POWER2008-60031.
[26] J.D. Beckham, A.K. Williamson, Salt-dome locations in the Gulf coastal plain, south-central United States, in: U.S. Geological Survey Water Resources Investigations Report 90, 1900, pp. 40–60, https://doi.org/10.3133/wri904060.
[27] S.C. Thieling, J.S. Moody, Atlas of shallow Mississippi salt domes, in: Bulleting 131 Mississippi Department of Environmental Quality, Geology, Office of, 1997. https://www.mdeq.ms.gov/wp-content/uploads/2017/06/Bulletin-131.pdf. (Accessed 2 February 2023).
[28] Geologic Study Southern Louisiana Salt Domes, Volume III. https://ntrl.ntis.gov/NTRL/dashboard/searchResults/titleDetail/TID28921.xhtml, 1979. (Accessed 2 February 2023).
[29] L.F. Dellwig, J.E. Bare, A radar investigation of north Louisiana salt domes, Photogramm. Eng. Remote. Sens. 44 (11) (1978) 1411–1419.
[30] L.M. Ruiz Maraggi, L. Moscardelli, G., Modeling hydrogen storage capacities, injection and withdrawal cycles in salt caverns: introducing the GeoH2 salt storage and cycling app, International Journal of Hydrogen Energy (2023), https://doi.org/10.1016/j.ijhydene.2023.03.293.
[31] J. Scafidi, M. Wilkinson, S. Gilfillan, N. Heinemann, S. Haszeldine, A quantitative assessment of the hydrogen storage capacity of the UK continental shelf, Int. J. Hydrogen Energy 46 (12) (2021) 8629–8639, https://doi.org/10.1016/j.ijhydene.2020.12.106.
[32] L. Lankof, R. Tarkowski, GIS-based analysis of rock salt deposits' suitability for underground hydrogen storage, Int. J. Hydrogen Energy 48 (71) (2023) 27748–27765, https://doi.org/10.1016/j.ijhydene.2023.03.415.
[33] D. Parkes, D.J. Evans, P. Williamson, J.D.O. Williams, Estimating available salt volume for potential CAES development: a case study using the Northwich Halite of the Cheshire Basin, Journal of Energy Storage 18 (2018) 50–61, https://doi.org/10.1016/j.est.2018.04.019.
[34] Python-visualization, Folium, Retrieved from, https://python-visualization.github.io/folium/, 2020.
[35] G. Van Rossum, F.L. Drake Jr., Python Reference Manual, Centrum voor Wiskunde en Informatica Amsterdam, 1995.
[36] P. Bérest, B. Brouard, M. Karimi-Jafari, L. Van Sambeek, Transient behavior of salt, Int. J. Rock Mech. Min. Sci. 44 (5) (2007) 767–786, https://doi.org/10.1016/j.ijrmms.2006.11.007.
[37] P. Berest, A. Réveillère, D. Evans, M. Stöwer, Review and analysis of historical leakages from storage cavern wells, in: Oil & Gas Science and Technology-Rev. IFP Energies nouvelles 74, 2019, p. 27, https://doi.org/10.2516/ogst/2018093.
[38] M. Bruno, Geomechanical Analysis and Design Consideration for Thin-Bedded Salt Caverns. Technical Report. OSTI identifier 850502, 2005, https://doi.org/10.2172/850502.
[39] A. Gillhaus, P.L. Horvath, Compilation of geological and geotechnical data of worldwide domal salt deposit and domal salt cavern fields, in: Solution Mining Research Institute Research Project Report 2007-1-SMRI, 2008.
[40] R.B. Gupta, A. Basile, T.N. Veziroğlu, Compendium of hydrogen energy volume 2: hydrogen storage, transportation and infrastructure, Woodhead Publishing Series in Energy 2016 (2016) 91–115, https://doi.org/10.1016/B978-1-78242-362-1.00004-3.
[41] M.I.T. Cavern, Texas Railroad Commission, in: https://www.rrc.texas.gov/oil-and-gas/applications-and-permits/injection-storage-permits/cavern-storage/cavern-storage-permit-procedures. (Accessed 7 December 2023).
[42] E. Lemmon, M.L. Huber, J.W. Leachman, Revised standardized equation for hydrogen gas densities for fuel consumption applications, J. Res. Natl. Inst. Stand. Technol. 113 (2008) 341–350, https://doi.org/10.6028/jres.113.028.
[43] E.W. Lemmon, I.H. Bell, M.L. Huber, M.O. McLinden, NIST Standard Reference Database 23: Reference Fluid Thermodynamic and Transport Properties-REFPROP, Version 10.0, National Institute of Standards and Technology, Standard Reference Data Program, Gaithersburg, 2018, https://doi.org/10.18434/T4/1502528.
[44] Louisiana Clean Energy. https://www.airproducts.com/louisiana-clean-energy. Accessed 3 June 2023.
[45] Brad Carl, Hy Stor Energy Strategic Partnership with Key Gulf Coast Port Becomes First to Deliver Renewable Hydrogen Access for Manufacturing, Industrial Applications, Port Operations and Long Duration Energy Storage. June 29. https://www.businesswire.com/news/home/20220629005311/en/Hy-Stor-Energy-Strategic-Partnership-with-Key-Gulf-Coast-Port-Becomes-First-to-Deliver-Renewable-Hydrogen-Access-for-Manufacturing-Industrial-Applications-Port-Operations-and-Long-Duration-Energy-Storage%20%20%20, 2022 (Accessed 3 June 2023).